ABOUT LIVER MACROSCOPIC FAILURE IDENTFICATION UNDER COMPRESSION

Cécile Conte, Pierre-Jean Arnoux, Nicolas Cheynel and Catherine Masson
Laboratoire de Biomécanique Appliquée, UMRT24: IFSTTAR/Université de la Méditerranée
Bd P. Dramard, 13916 MARSEILLE Cedex 20, FRANCE
Corresponding author email: cecile.conte@ifsttar.fr

SUMMARY
To provide a better understanding and modeling of liver trauma, an experimental study of its behavior under dynamical compression loading had been done. A method was developed to identify failure in the force signal using its derivative form. Then, estimations of injury criterion for liver in compression are proposed, and the influence of loading velocity is analysed.

INTRODUCTION
To prevent abdominal organs traumas in car crash situations, the definition of efficient safety devices should be based on a detailed knowledge of human tolerance, i.e. injury mechanisms and related injury criteria [1]. This knowledge should be based on experimental observation of these mechanisms throw damage and failure analysis.

Among all abdominal organs, the liver is one of the most frequently injured, because of its important size, weight and critical location. In car crash situations, liver injuries seem to be obtained by dynamic compression during the brutal body deceleration [2]. Some authors have described this global dynamical behaviour in compression [3-5] but not really analysed damage and failure occurrence into the structure.

Hence, this work aims to investigate damage and failure process of the human liver under trauma loading from quasi-static to dynamic uniaxial compression tests. Mechanical behaviour investigations are then completed by a failure occurrence analysis to understand the injury mechanisms.

METHODS
Fifteen livers were removed from embalmed post mortem human subjects (PMHS) obtained from the Marseille Faculty of Medicine. The PMHS (6 males and 9 females) were between 65 and 93 years old.

Livers were uniformly compressed between two steel plates at four different velocities until reaching 60% of their initial thickness. Load was applied along the anterior-posterior organ axis using a hydraulic cylinder MTS 370.10 axial 15 KN. Compression plates were larger than livers dimensions to avoid border effects (Figure 1) and were coated with petroleum jelly to limit friction with organ surface. The four compression velocities were 0.0013 (3 livers), 0.01 (4 livers), 0.2 (4 livers) and 1 m/s (4 livers). Data recorded during each test were the upper plate displacement (LVDT MTS 390751-03, nominal capacity: 100 mm, precision: 0.04 mm) and the force transmitted by the organ (force cellule MTS 661.19H-03, nominal capacity ±15 kN, precision: ±10 N). Acquisition frequency for both measures was 1024 Hz. Additionally, front and rear views of the test were obtained using high speed movies (1000 pictures /second).

Figure 1: Experimental compression set-up.

Injury analysis was performed after each test. Force signal was derived to amplify its variations. Temporal location of anomalies of this derived curve was compared to injuries occurrence in the video recordings.

RESULTS AND DISCUSSION
Liver global behavior in compression exhibits the same steps whatever the loading velocity. First an elastic phase shows a linear variation of force with relative displacement (defined as the ratio between upper plate displacement and initial liver thickness). Then a densification phase is observed, that is first non linear and reaches a quasi-linear stage before experiencing damage and failure (Figure 2). This global hyperelastic behavior is relevant with previous works reported on abdominal soft tissues [4, 5].

As the damage occurrence cannot be directly deduced from force-displacement curve, the force derivative is computed. The obtained curve shows huge peak-shaped anomalies (Figure 2). As movies analysis exhibits a matching between these peaks times and the observed injuries occurrence, these peaks are postulated as indicators of failure occurrence in the force signal. Thus the following assumption is made: the break of slope point of the derivative force curve observed before the peaks is the first macroscopic failure event within the organ (Figure 2 and Table 1). Failure then occurs for a lower compression level for high velocities tests (0.2 and 1 m/s) than

for low ones (0.0013 and 0.01 m/s). Moreover, two ultimate strains (expressed by the relative displacement) can be deduced. Their values are of 43% for low velocities and 34% for high velocities. Ultimate force levels show large scatter according to the different livers tested.

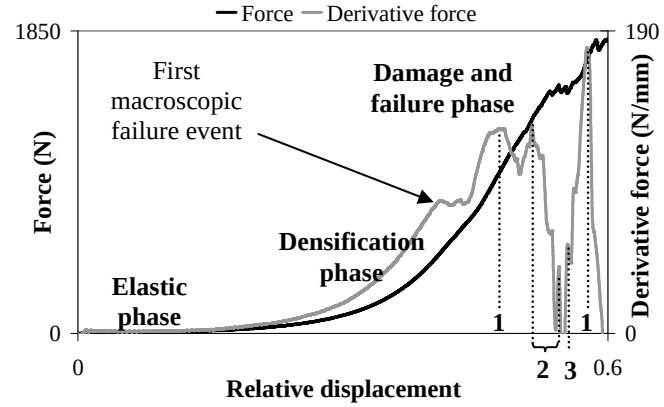

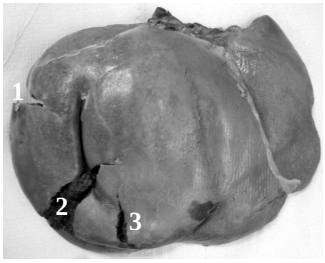

1. Two step laceration of the lateral face.
2. Progressive laceration of the inferior face.
3. Sharp laceration of the inferior face

Figure 2: Force and derivative force curves and injury analysis of a liver tested at 0.01 m/s. Numbers figure both the injury observed and the matching peaks of the derivative force.

With our assumption, the failure is postulated for a significant variation of derivative force curve corresponding to a significant failure event. But damage and micro-failure may occur earlier without any detectable incidence on the recorded force. Hence each of the deduced ultimate strains could be considered as the upward estimation of a failure criteria in each velocity class. These estimated criteria have to be considered as macroscopic data. Further tests with reduced amplitude of compression should then be performed to evaluate the local damage and associated damage criteria.

These experimental results could show dependency on the testing conditions. First of all, using cadaveric organs create discrepancy because there is no more fluid within the vascular structures [6] and also because of conservation [7]. In our case, a histological analysis showed that the conservation did not alter the tissue structure in a significant way. The loading conditions used in this work were chosen 10 and 2 times lower than the effective speed of the liver during a crash [8]. This assumption was performed in order to consider the global abdominal damping effects.

CONCLUSIONS

This work describes both a method to localize compression injuries in a force signal and an analysis of the failure occurrence during a trauma compression of human liver. The results lead to postulate two ultimate strains for both low and high velocities. They then constitute a first estimation of strain rate dependant macroscopic injury criteria. In a further step, injury occurrence will be observed at the histological level through damage analysis. Finally, this work aims to be used to improve liver numerical models used for injury prediction and analysis in car crash conditions.

REFERENCES

1. Haug E, et al. Human Models for Crash and Impact Simulation, *Handbook of Numerical Analysis*. **12**: 231-452, 2004.
2. Cheynel N, et al. Comparison of the biomechanical behavior of the liver during frontal and lateral deceleration, *Journal of Trauma*. **67(1)**: 40-4, 2009.
3. Melvin JW, Stalnaker RL and Roberts VL. Impact injury mechanisms in abdominal organs, *SAE Transactions*. 115-126, 1973.
4. Miller K. Method of testing very soft biological tissues in compression, *Journal of Biomechanics*. **38(1)**: 153-158, 2005.
5. Sparks JL, et al. Using Pressure to Predict Liver Injury Risk from Blunt Impact, *Stapp Car Crash Journal*. **51**: 401-432, 2007.
6. Kerdok AE, Ottensmeyer MP and Howe RD. Effects of perfusion on the viscoelastic characteristics of liver, *Journal of Biomechanics*. **39(12)**: 2221-2231, 2006.
7. Crandall JR and Pilkey WD. The Preservation of Human Surrogates for Impact Studies. Proceedings of 13th Southern Biomedical Engineering Conference, Washington, Engineering Research Center, University of DC, 1994.
8. Viano DC, et al. Biomechanics of the human chest, abdomen, and pelvis in lateral impact, *Accident Analysis & Prevention*. **21(6)**: 553-574, 1989.

Table 1: Influence of loading velocities on the ultimate displacement and force data deduced from the first failure point.

Loading velocity (m/s)	Relative displacement at the first failure time (%)	Reached force at the first failure time (N)
0.0013	43.6 ± 7.1	311 ± 55
0.01	47.3 ± 6.4	1 601 ± 963
0.2	34.1 ± 5.1	1 077 ± 89
1	37.3 ± 10.4	1 616 ± 760